Journal of Chromatography A, 1603 (2019) 348–354

Contents lists available at ScienceDirect

Journal of Chromatography A

journal homepage: www.elsevier.com/locate/chroma

Modeling the competitive adsorption of sample solvent and solute in supercritical fluid chromatography

Csanád Rédei [a], Attila Felinger [a,b,c,*]

[a] Department of Analytical and Environmental Chemistry and Szentágothai Research Center, University of Pécs, Ifúság útja 6, H-7624 Pécs, Hungary
[b] MTA-PTE Molecular Interactions in Separation Science Research Group, Ifúság útja 6, H-7624 Pécs, Hungary
[c] Institute of Bioanalysis, University of Pécs, Szigeti út 12, H-7624 Pécs, Hungary

ARTICLE INFO

Article history:
Received 18 April 2019
Received in revised form 20 May 2019
Accepted 23 May 2019
Available online 25 May 2019

Keywords:
Supercritical fluid chromatography
Competition
Solvent effects
Inverse method
Displacement effect

ABSTRACT

Uncommon retention behavior of a series of *n*-alkylbenzene homologues as well as the effect of different sample solvents on chromatographic efficiency were studied in supercritical fluid chromatography. After testing various columns, an alkylamide stationary phase was selected for detailed studies. The results showed that even a small amount of methanol originating only from the sample, overloaded the column and competitive adsorption was induced between the analytes and the sample solvent for adsorption on the stationary phase. This was indicated by the changes in column efficiency, retention and peak widths. The concentration of the analytes in the sample was negligible compared to the amount of methanol – but their adsorption was influenced by the solvent – while the adsorption of methanol remained unaffected by the *n*-alkylbenzenes. First, the competition was described by determining the single-component adsorption isotherms for both the analytes and their solvent, then competitive isotherms were calculated. Based on the peak profiles, bi-Langmuir and competitive bi-Langmuir isotherms were assumed. The solvent effect was modeled by a numerical method created in-house where the differential mass balance equation given by the equilibrium–dispersive (ED) model was integrated using the Rouchon algorithm. The experimental observations were confirmed by *in silico* experiments and additional cases involving two hypothetical analytes were studied as well.

1. Introduction

Supercritical fluid chromatography (SFC) has gathered increased attention over the last few years in the fields of both analytical [1,2] and preparative chromatography [3–6], theoretical research (*e.g.* the effects of sample diluent [7], mobile phase density [8], modifier adsorption [9,10]), as well as forensics [11], chiral separations [12] and numerous other areas of application including the pharmaceutical [13] and food industry [14]. Its growing reputation can be associated with the rapid technological advancements of the last decade that make SFC a highly viable and comparable, but ultimately a complementary technique besides liquid chromatography (LC).

SFC is usually characterized by having three major advantages over LC that stem from the physico-chemical properties of carbon dioxide: (1) it is cheaper and more environmentally friendly compared to LC due to lower organic solvent consumption, (2) the low viscosity of the mobile phase enables higher flow-rates and thus shorter separations and also permits rapid diffusion processes, reduced band broadening effects hence increased efficiency and (3) eluent strength is considered to be "well-tunable" by adjusting temperature, pressure and the concentration of the organic modifier in the mobile phase. However, it is important to note that depending on the experimental conditions, some of the advantageous properties may not be achieved at the same time, rather a compromise has to be made [15].

Recently, Gritti reported unexpected retention phenomena of a series of *n*-alkylbenzenes in SFC resulting in shifts in retention, band compression and enlargement [16]. He found that the sample solvent overloaded the C_{18} column and the solvent band divided the chromatogram into three parts, each with different efficiency results. Analytes less retained than the solvent showed similar column efficiencies as if there was no solvent-analyte band interference. In the case of more retained analytes, decreased column efficiencies were observed due to band enlargement and when both

* Corresponding author at: Department of Analytical and Environmental Chemistry and Szentágothai Research Center, University of Pécs, Ifúság útja 6, H-7624 Pécs, Hungary.
E-mail address: felinger@ttk.pte.hu (A. Felinger).

https://doi.org/10.1016/j.chroma.2019.05.045
0021-9673/

retentions matched closely, the interference resulted in extremely high apparent efficiencies as a result of band compression.

Similar phenomena have been reported for the first time by Nilsson and Westerlund in reversed phase ion pair liquid chromatography [17]. Besides the analytes, the sample also contained high concentrations of an organic anion that formed ion pairs with a cationic component of the mobile phase. This created a zone with a different composition compared to the bulk mobile phase in the column that induced similar behavior, including band compression, as mentioned above.

Choosing the most suitable sample solvent in SFC can be challenging during method development. Unfortunately, the mobile phase cannot be used since it mainly consists of pressurized carbon dioxide that becomes gaseous at room temperature and atmospheric pressure, therefore a proper liquid has to be selected. Very often the analytes are dissolved in solvents or solvent mixtures imitating the polarity of the mobile phase which the compounds are highly soluble in. Another option is to use the modifier as the solvent. These, however, can lead to solvent–mobile phase mismatches due to solvent strength and viscosity differences that are often detrimental to peak profiles [18]. If neat carbon dioxide with no modifier is used as mobile phase, competition between the solutes and the sample solvent can also occur for the adsorption sites of the stationary phase that has additional adverse effects on peak integrity [9].

In this study, uncommon retention behavior of *n*-alkylbenzenes is presented caused by competition between the sample solvent and the analytes for adsorption on the stationary phase. A numerical method is proposed to model the competition and perform simulations for theoretical cases. Accurate mass flow-rate measurements of the mobile phase have been carried out since high column temperatures have been used where the difference between set and actual volumetric flow-rates is more prevalent. Single-component and competitive adsorption isotherms have been calculated to assemble the model and confirm the experimental results. Finally, *in silico* experiments were performed for two theoretical cases then the results were explained.

2. Theory

2.1. Adsorption isotherms

In order to describe the competition between the analytes and the sample solvent, their single-component equilibrium isotherms have to be known. The adsorbent surface of the column can be considered nonhomogeneous, thus the different adsorption energy sites need to be accounted for. For this purpose the bi-Langmuir isotherm was used during the calculations, which is the simplest model for a heterogeneous surface where the adsorption energy distribution is considered bimodal [19]. The adsorbent surface is assumed to be a combination of two different homogeneous surfaces:

$$q_i = \frac{a_1 C_i}{1 + b_1 C_i} + \frac{a_2 C_i}{1 + b_2 C_i} \tag{1}$$

where q_i and C_i are concentrations of component i in the stationary and mobile phases, respectively; a_1 is the initial slope of the isotherm, b_1 the equilibrium constant for one of the sites and a_2 and b_2 are the same parameters for the other site, respectively [19].

The bi-Langmuir isotherm can be extended to multicomponent systems. However, when multiple compounds are present in the sample, they interfere and compete for adsorption. In addition, competition is not limited only to the analytes but can also occur between the sample solvent and the analytes. This is especially true for SFC, where the sample cannot be prepared with the use of the mobile phase. If the surface is nonhomogeneous and the compounds follow bi-Langmuir isotherm behavior then the competition can be described with the competitive bi-Langmuir isotherm as

$$q_i = \frac{a_{i,1} C_i}{1 + b_{A,1} C_A + b_{B,1} C_B} + \frac{a_{i,2} C_i}{1 + b_{A,2} C_A + b_{B,2} C_B} \tag{2}$$

where C_A and C_B are concentrations of component A and B in the mobile phase and the other coefficients are the same as those obtained for the single-component isotherms of the two compounds [19].

2.2. Determination of adsorption isotherms

The inverse method (IM) is one of several methods available aiming to solve the general inverse problem of chromatography where the column response, the mass-balance equation, the initial and boundary conditions are known and the experimental elution profiles are assumed to be solutions of the column model [20]. Unlike the other approaches, the isotherm model has to be selected in advance and the initial isotherm parameters are estimated with the help of an analytical injection and another method used in isotherm determination. The next step is the calculation of overloaded band profiles by integration of a chosen mass balance equation. Then the following objective function is used to compare the measured and calculated band profiles:

$$\min \sum_i r_i^2 = \min \sum_i (C_i^{\mathrm{sim}} - C_i^{\mathrm{meas}})^2 \tag{3}$$

where C_i^{sim} and C_i^{meas} are calculated and measured concentrations at point i and r_i is their difference. The last step is the minimization of the objective function through the adjustment of the isotherm parameters with the help of an optimization algorithm [21–23].

Estimation of the initial isotherm parameters can be performed *e.g.* with the elution by characteristic point (ECP) method. In this approach the isotherm is generated from the diffuse rear part of the overloaded band profile by integrating the peak area starting from the tail end until the peak maximum that serves as the characteristic point [3]. The isotherm can be calculated using partial sums as follows:

$$q(C) = \frac{1}{V_a} \int_0^C (V - V_0) \mathrm{d}C \tag{4}$$

where $q(C)$ is the amount adsorbed on the stationary phase when it is in equilibrium with concentration C, V_a is the volume of the adsorbent, V is the retention volume of the point in the rear part of the profile at concentration C or characteristic point and V_0 is the hold up volume of the column. Each point of the rear profile gives one point of the isotherm, however the method is derived from the ideal model that assumes infinite column efficiency. Therefore, the estimation is only applicable with highly efficient columns. In addition, the model assumes rectangular injection profiles but the resulting error can be decreased by injecting small amounts [20]. Another source of systematic error can be caused by the selection of the starting and ending points of the integration. Although there have been some improvements for ECP that eliminate most of the drawbacks [24,25], the method was strictly used for rough initial estimation in this study.

An accurate mass balance equation can be given by the equilibrium–dispersive (ED) model when mass transfer kinetics are controlled only by very fast molecular diffusion effects. The model assumes constant equilibrium between the mobile and stationary phases and band-broadening effects including axial dispersion and the finite rate of mass transfer kinetics is incorporated in an

apparent dispersion term. The mass balance equation for each component can be given as:

$$\frac{\partial C_i(z,t)}{\partial t} + F\frac{\partial q_i(z,t)}{\partial t} + u\frac{\partial C_i(z,t)}{\partial z} = D_a\frac{\partial^2 C_i(z,t)}{\partial z^2} \quad (5)$$

where z is the distance along the column, t the time, u the mobile phase linear velocity and F the phase ratio with

$$F = \frac{1-\varepsilon_t}{\varepsilon_t} \quad (6)$$

where ε_t is the total porosity of the column. D_a is the apparent dispersion coefficient that can be calculated from an analytical elution profile and is given with

$$D_a = \frac{uL}{2N} = \frac{Hu}{2} \quad (7)$$

where N is the number of theoretical plates and H is the plate height. The initial condition

$$C_i(z,0) = 0 \quad (8)$$

states that at $t = 0$ the column is equilibrated with the mobile phase in which the concentration of the solute is zero. The boundary condition (*i.e.* the injection profile) for each component can be written as:

$$C_i(0,t) = C_i^0 \quad (9)$$

$$0 < t \leq t_p \quad (10)$$

where t_p is the injection time. In some cases, the injection profile may be assumed to be rectangular with a length of t_p, however this assumption is incorrect in most practical applications [20,21]. The inlet profile of the injection has a major effect on band profile and should be known accurately. Therefore, in this study the actual injection profile was obtained from an analytical injection where the column was replaced with a zero volume connector.

The differential mass balance equation defined in Eq. (5) neglects the compressibility of the mobile phase. Therefore, it has limited applicability in SFC where the pressure gradient along the column alters the density of the mobile phase and eventually its elution strength. Nevertheless, when pressure drop along the column is only moderate, Eq. (5) gives an accurate estimation of the band profiles.

3. Experimental

3.1. Chemicals

Carbon dioxide with a purity of 99.5% was purchased from Linde (Répcelak, Hungary). HPLC grade benzene, acetonitrile, methanol and heptane were purchased from VWR International (Fourtenay-sous-Bois, France). The analytical standards ethylbenzene, butylbenzene, hexylbenzene, octylbenzene, decylbenzene, dodecylbenzene, tetradecylbenzene and octadecylbenzene were all purchased from Sigma-Aldrich (Steinheim, Germany) with a minimum purity of 99%.

3.2. Instruments

All experiments were performed using a Waters ACQUITY UPC^2 system (Milford, MA, USA). The instrument was equipped with a binary solvent delivery pump, an autosampler with a 10 μL sample loop, a column thermostat, a photodiode array detector and a back pressure regulator. Instrument control and data management were performed by Empower 3 software. The extra-column volume of the instrument was 0.055 cm^3 from the loop to the detector cell and was measured by replacing the column with a zero-volume connector. All retention volumes were corrected for this contribution.

Accurate CO_2 mass flow-rates were measured with a mini CORI-FLOW mass flow meter from Bronkhorst High-Tech B.V. (Ruurlo, Netherlands), Model No. M13-ABD-11-0-S, Serial No. B11200776A. This model provides an accuracy of ±(0.2% of the read value + 0.5 g/h), which translates to a sensitivity of 0.01 g/min of CO_2.

Calculation of the mobile phase densities was based on the column thermostat temperature and the inlet and outlet pressures of the column measured directly using an external pressure gauge (OMEGA Engineering, Norwalk, CT, USA). The densities were calculated using the NIST REFPROP database.

The mean volumetric flow-rate $\overline{F}_v$ was estimated from the mass flow-rate of the mobile phase F_m measured downstream the mixer and the average density $\overline{\rho}$ calculated as the arithmetic mean of the densities at the inlet and outlet of the column as follows:

$$\overline{F}_v = \frac{F_m}{\overline{\rho}} \quad (11)$$

However, individual volumetric flow-rates for the inlet and outlet of the column can also be calculated. Based on the measured data, flow-rate at the inlet was $F_{v,in}$ = 1.16 mL/min and $F_{v,out}$ = 1.20 mL/min at the outlet at 60 °C temperature and 150 bar back pressure. The reason for these specific experimental parameters is explained in Section 4.1. The difference in flow-rates is interesting but not unexpected. Because of the adiabatic expansion of carbon dioxide along the column, a higher mobile phase velocity at the outlet of the column can be expected.

It has been shown that there is a difference between set and actual experimental parameters in SFC. However, in the case of moderate temperatures, the column thermostat setting can be a good approximation of the actual conditions [20,26]. At the time of the experimental work, no temperature sensors were available for accurate measurements at the column inlet and outlet, therefore accuracy of the temperature data could not be determined. The column was equilibrated for 60 min at every set temperature in order to introduce the smallest error possible to the model.

3.3. Chromatographic experiments

All measurements were carried out with 100% CO_2 mobile phase. The flow-rate was set at 1.00 mL/min, the actual flow-rate was calculated to be 1.18 mL/min at 60 °C and 150 bar back pressure. Column temperature was varied between 35 and 60 °C, the back pressure regulator was set at either 105, 150 or 200 bar. The injection volume was 2.0 μL. The detector signal of the alkylbenzenes was recorded between 190 and 400 nm, the optimal channels were 260 and 273 nm.

The samples contained benzene, ethylbenzene, butylbenzene, hexylbenzene, octylbenzene, decylbenzene, dodecylbenzene, tetradecylbenzene and octadecylbenzene dissolved in either acetonitrile, methanol or heptane. The concentrations were set at 0.5, 0.7, 1.1, 1.8, 2.2, 3.4, 4.5, 5.0 and 5.4 g L^{-1}, respectively.

During the preliminary tests, several stationary phases were tested for uncommon retention behavior. The columns involved were Zorbax Eclipse Plus C18, SB-C8 and C18 (3.5 μm, 4.6 × 150 mm) from Agilent Technologies (Palo Alto, CA, USA), Synergi MAX-RP (4 μm, 4.6 × 150 mm) from Phenomenex (Torrance, CA, USA), Ascentis Express C18 (2.7 μm, 2.1 × 50 mm) from Supelco–Sigma–Aldrich (Bellefonte, PA, USA), Symmetry C8 and C18 (3.9 and 4.6 × 150 mm, respectively) from Waters and Kromasil C18 (5 μm, 4.6 × 150 mm).

Ultimately, a 4.6 × 150 mm Supelcosil ABZ+Plus alkylamide column packed with 3 μm particles from Supelco–Sigma–Aldrich was chosen for further studies. The total volume of the column was

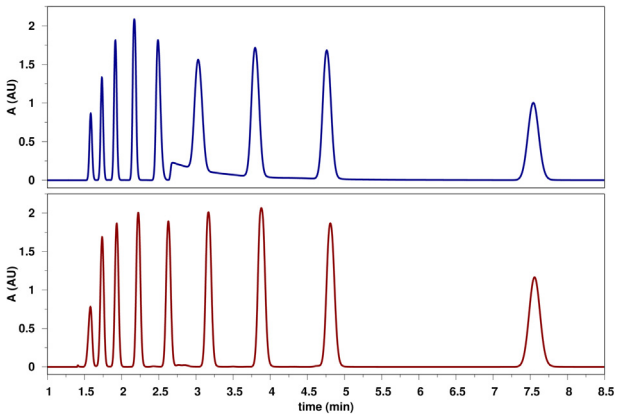

Fig. 1. Chromatograms of *n*-alkylbenzenes in methanol (top) and heptane (bottom) obtained with the alkylamide column, neat CO_2 mobile phase, 200 nm, 60 °C and 150 bar BPR. Note the overloaded solvent band of methanol starting at $t = 2.65$ min.

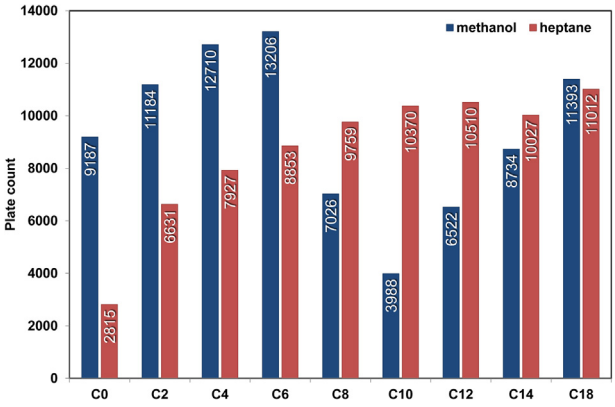

Fig. 2. The effect of methanol and heptane sample solvents on column efficiency. The negative effect of the former is prevalent in the case of octylbenzene, decylbenzene and dodecylbenzene, however hexylbenzene and below showed increased efficiency due to band compression.

$V_{tot} = 2.492$ cm^3. The void volume was estimated by two methods, the weight-difference method that usually gives an underestimation and with the help of heptane used as an unretained marker [27]. Both approaches gave very similar results so $V_0 = 1.590$ cm^3 was used in the end. Total porosity was calculated to be $\varepsilon_t = 0.638$.

4. Results and discussion

4.1. The effect of different sample solvents

Screening measurements for all stationary phases were performed with the three different samples containing either acetonitrile, heptane or methanol as solvent. The purpose of the experiments was to find *detectable* solvent adsorption that had an effect on the retention mechanism of the analytes with neat carbon dioxide mobile phase. In the case of acetonitrile and heptane, no such phenomenon could be identified on any of the columns.

Methanol, however, overloaded the alkylamide column and exhibited a strong, detectable adsorption. By adjusting temperature and pressure, the relative retention of the solvent and the analytes was influenced in a way that the chromatogram would be divided into two parts around the middle. This was achieved with 60 °C temperature and 150 bar back pressure. Fig. 1 shows the experimental chromatograms obtained in methanol (top) and heptane (bottom). The top graph shows a well-defined band of methanol starting at around $t = 2.65$ min that was confirmed by single injections of the solvent.

Comparing the two chromatograms, the changes in column efficiency, retention times and peak widths are rather distinct and are caused by competitive adsorption of methanol and the alkylbenzenes for the adsorption sites. Column efficiency was characterized by the number of theoretical plates acquired by fitting exponentially modified Gaussian functions (EMG) to the experimental data. The fitting was performed in PeakFit v4.12 software.

One can observe in Fig. 2 that when the sample is dissolved in heptane, the number of theoretical plates continuously increases along the homologous series. When the sample solvent is methanol, however, a significantly larger efficiency is observed for homologues smaller than octylbenzene compared to the efficiency when heptane is the sample solvent. This is caused by the displacement effect that the large amount of methanol induces; as methanol displaces the alkylbenzenes, a peak focusing, sharpening is observed. Then, for the later eluting alkylbenzenes, the efficiency suddenly drops due to the tag-along effect induced again by methanol. The retention time of octadecylbenzene is large enough so the efficiency for that compound is not disturbed by the adsorption of the sample solvent methanol.

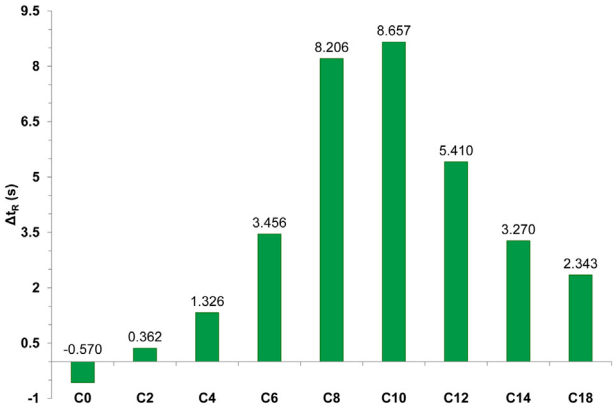

Fig. 3. Shifts in retention times in the case of methanol solvent, where the chromatogram obtained in heptane was used as reference for the calculation. Positive values mean a decrease in retention time in seconds. The results for benzene should be disregarded due to its very low retention resulting in a close proximity to the system peaks.

A closer look on efficiency (see Fig. 2) and retention times (see Fig. 3) further supports the assumption and shows that the most affected compounds were around the maximum of the methanol band, namely octylbenzene and decylbenzene. Accordingly, further calculations and simulations focused on this part of the chromatogram.

4.2. Single-component isotherms

Overloaded band profiles of methanol, octylbenzene and decylbenzene were recorded for the purpose of determining the single-component isotherms by the inverse method. The two alkylbenzenes could not be properly dissolved in methanol to obtain a sample with high enough concentration, so injections of the neat standards were performed instead. Calculations required concentration profiles rather than the original, absorbance versus time profiles, therefore calibration of the detector was necessary.

We chose a linear calibration approach so the wavelength of 273 nm was selected for the recorded chromatograms of alkylbenzenes to remain in the linear range of the detector response. By

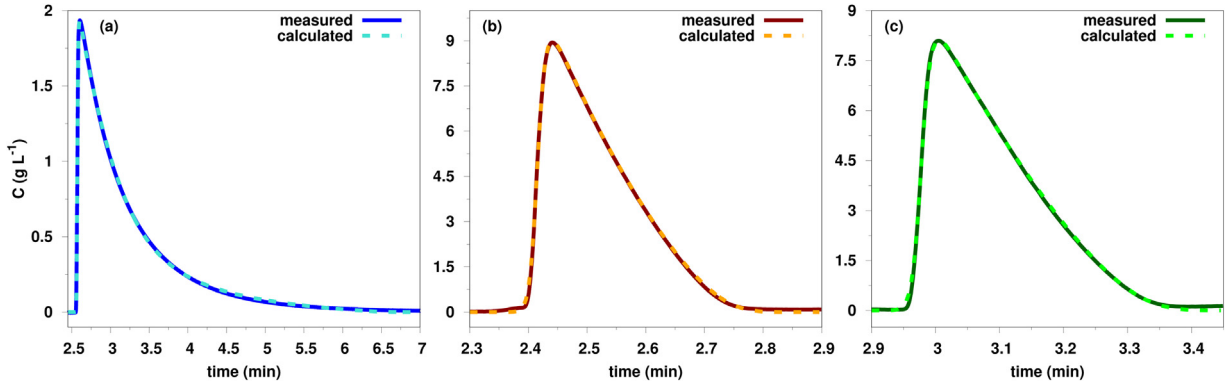

Fig. 4. Measured and calculated profiles obtained by the inverse method for methanol (a), octylbenzene (b) and decylbenzene (c). The agreement is very good, proving the bi-Langmuir isotherm is a suitable choice to model the adsorption energy distribution of the heterogeneous surface.

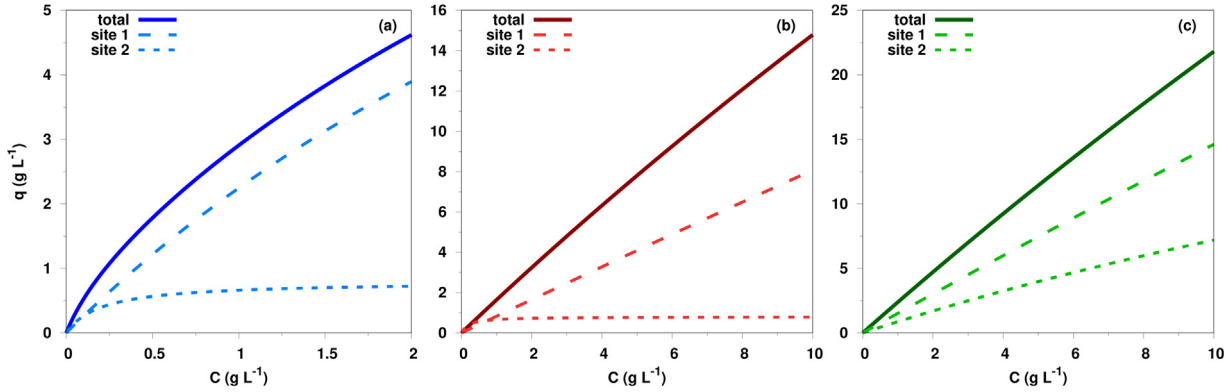

Fig. 5. Isotherm curves of methanol (a), octylbenzene (b) and decylbenzene (c). Note how methanol enters the nonlinear range of the isotherm while the alkylbenzenes mainly remain in the linear range due to severe dilution after the injection process. Behavior of the two different sites is also noteworthy.

integrating the elution profile, the amount of the injected sample m_{inj} can be obtained:

$$m_{inj} = \int C(V)\mathrm{d}V = \overline{F}_v \int C(t)\mathrm{d}t \tag{12}$$

Absorbance is proportional to concentration in the linear range of the detector signal. The relation can be expressed with a sensitivity factor κ as follows:

$$A(t) = \kappa C(t) \tag{13}$$

$$A_T = \int A(t)\mathrm{d}t \tag{14}$$

$$A_T = \kappa \int C(t)\mathrm{d}t = \frac{\kappa m}{\overline{F}_v} \tag{15}$$

$$\kappa = \frac{A_T \overline{F}_v}{m} \tag{16}$$

where A_T is the peak area. With κ determined, concentration is easily obtained as:

$$C(t) = \frac{A(t)}{\kappa} \tag{17}$$

Absorbances of methanol, octylbenzene and decylbenzene were transformed into concentrations with the above method.

The initial isotherm parameters were estimated numerically with the ECP method. The algorithm calculated isotherm curves from the diffuse rear parts of the chromatograms as well as the void and adsorbent volumes of the column. The parameters were obtained by fitting the bi-Langmuir isotherm on the output curves.

Table 1
Single-component isotherm parameters determined by the inverse method.

	Methanol	Octylbenzene	Decylbenzene
a_1	2.652	0.828	1.521
b_1 (L g^{-1})	0.181	0.003	0.004
$q_{s,1}$ (g L^{-1})	14.671	317.222	374.596
a_2	3.895	0.833	0.890
b_2 (L g^{-1})	4.885	0.024	0.024
$q_{s,2}$ (g L^{-1})	0.797	34.736	37.579
FSSR	0.661	2.947	2.919

The inverse method was applied to the overloaded band profiles of the three compounds to accurately determine their single-component adsorption isotherms. The calculations were performed by a numerical method where the differential mass balance equation given by the ED model was integrated by the Rouchon algorithm. The method employed a nonlinear simplex algorithm to determine the isotherm parameters. Besides the overloaded profiles, the initial isotherm parameters and the column parameters, the method also required the inlet profile of the injection that was recorded as described at the end of Section 2.2.

The measured and calculated profiles are plotted in Fig. 4 . The calculated data fits very well to the experimental profiles confirming the bi-Langmuir model was an appropriate choice for the heterogeneous surface with bimodal adsorption energy distribution. Table 1 summarizes the final isotherm parameters for the three compounds. The final sum of squared residuals (FSSR) is the variance of the fitting error that gives information about the goodness of the fit. The values further support the observations of Fig. 4 . The two adsorption sites, characterized by saturation capacities $q_{s,1}$

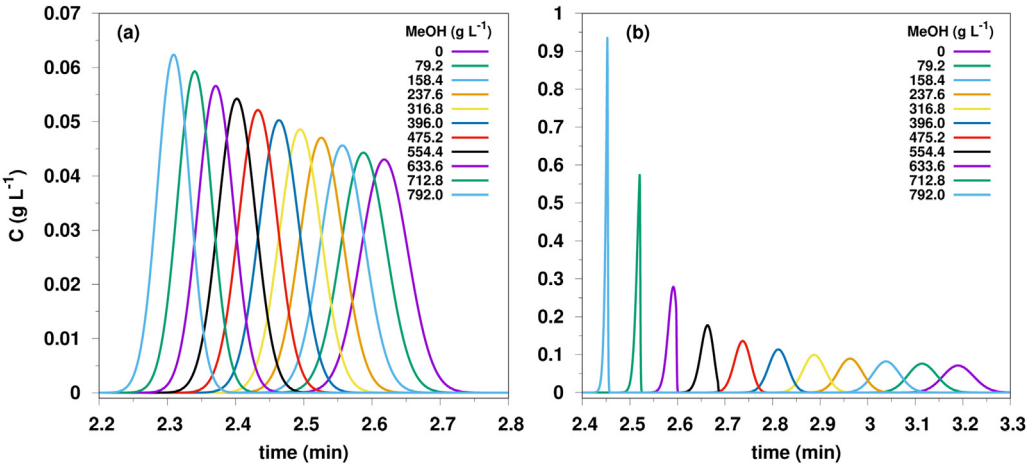

Fig. 6. Results of *in silico* experiments of octylbenzene (a) and decylbenzene (b). As methanol content increased, retention of the compounds decreased in both cases and the displacement effect could be observed.

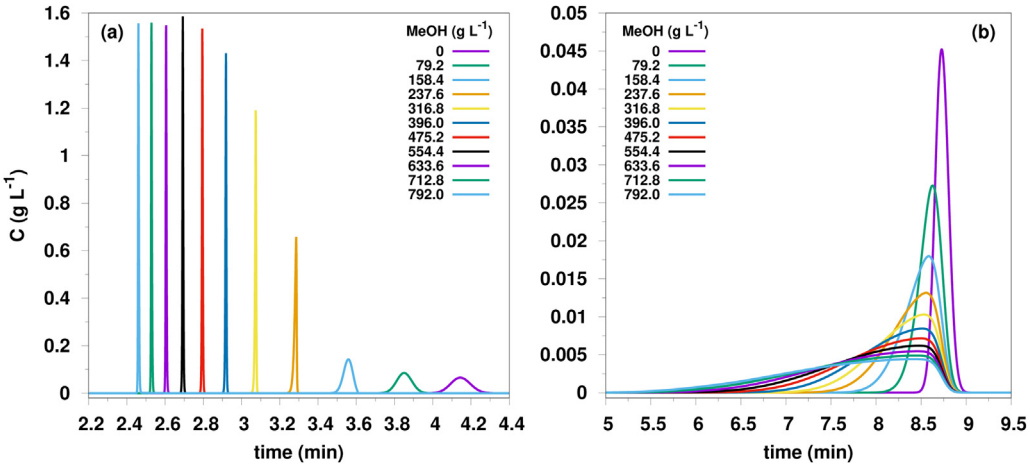

Fig. 7. Results of *in silico* experiments of hypothetical compounds H1 (a) and H2 (b). Retention decreased with increasing methanol content. While the displacement effect was observed in the case of H1, H2 was affected by the tag-along effect.

and $q_{s,2}$, respectively, showed similar behavior in all cases. All compounds exhibited a stronger affinity to site 1 during the adsorption process while site 2 was saturated early on. The isotherm curves along with the curves of the individual sites are plotted in Fig. 5 . The diffuse rear part of the methanol band resulted in site 2 reaching its maximum saturation capacity very quickly while the alkylbenzenes did not really enter the nonlinear range of the isotherm. This can be explained with the injected amount, containing only the neat compounds, undergoing a quick and severe dilution immediately after entering the column resulting in a two orders of magnitude decrease in concentration along the column.

4.3. Competitive isotherms

Competition of the individual alkylbenzenes against methanol was modeled with the competitive bi-Langmuir isotherm. The model was assembled from the previously determined single-component isotherm parameters using a similar numerical approach as previously. The algorithm calculated competitive isotherms and generated concentration versus time chromatograms. By changing the initial concentration parameters of the analyte and solvent, a wide range of cases can be investigated.

Fig. 6 shows how the retention and peak profiles of octylbenzene (left) and decylbenzene (right) changed with the amount of methanol. The initial alkylbenzene concentration was set to the actual concentrations of the sample injected during the preliminary studies (2.2 g L^{-1} for C_8 and 3.4 g L^{-1} for C_{10}), while the concentration of methanol was increased gradually from 0 to 792.0 g L^{-1} so the final step represented the real injections. In the actual sample, the concentration of the analytes was negligible compared to the amount of methanol, while their adsorption was influenced by the solvent. The adsorption of methanol, however, remained unaffected by the alkylbenzenes. During the simulations, the retention time of methanol was t_{MeOH} = 6.35 min, while for the alkylbenzenes at step 1, with no methanol present it was t_{C8} = 2.62 min and t_{C10} = 3.19 min.

In both cases, retention decreased as the concentration of methanol increased. In addition, band compression and in the case of decylbenzene, peak distortion could be observed. The observations can be linked to the displacement effect. Competition occurred in the nonlinear range of the isotherm resulting in methanol disturbing the adsorption of the analytes and ultimately acting as a displacing agent. In the case of decylbenzene, the competition induced overlapping bands with the solvent, producing abnormal peak shapes and apparent efficiency.

Two hypothetical solutes, H1 and H2, both set at 5.0 g L^{-1} concentration were also investigated by modifying the isotherm parameters a_1 and a_2. The retention time of H1 was set at t_{H1} = 4.15 min meaning a stronger retention than decylbenzene but weaker than methanol, while H2 was set at t_{H2} = 8.74 min which

meant a stronger retention than methanol. The changes in retention and peak shapes of H1 (left) and H2 (right) are illustrated in Fig. 7 .

H1 was affected by the same displacement effect but with a more severe outcome, displacement was more emphasized. H2, however, exhibited the tag-along effect caused by the abundance of the weakly adsorbing methanol, prohibiting the adsorption process of the compound by acting as an inhibitor and blocking access to the adsorption sites. This resulted in elongated bands and decreased apparent efficiency.

5. Conclusions

Competitive adsorption of the solute and solvent was investigated in supercritical fluid chromatography. A series of *n*-alkylbenzene homologues were chosen as model compounds along with acetonitrile, methanol and heptane as sample solvents. After a series of preliminary experiments, the phenomenon was successfully detected with an alkylamide column, at 60 °C temperature, 150 bar back pressure and neat carbon dioxide mobile phase. In the case of methanol, the competition was easily identified based on the decreased column efficiency, shifts in retention times and changes in peak widths, since the variation of these properties was highest around the methanol band.

Single-component isotherm were determined for methanol and two alkylbenzenes surrounding the solvent band. To account for the adsorption energy distribution of the heterogeneous surface of the stationary phase, the bi-Langmuir isotherm was selected and the parameters were determined by the inverse method using a numerical method where the differential mass balance equation given by the equilibrium–dispersive model was integrated by the Rouchon algorithm. The results showed a very good agreement between the experimental and calculated band profiles and the behavior of the two different adsorption sites were also explored, all compounds favored site 1 by around two orders of magnitude in terms of the saturation capacity.

The competitive bi-Langmuir isotherm was chosen to model the competition. The model employed the determined parameters and a similar numerical approach as before. A series of *in silico* experiments were performed where all solute concentrations were set in the analytical range and the amount of the solvent was increased step by step to imitate the real injections. Besides the alkylbenzenes, two hypothetical solutes (H1 and H2) were also investigated with varying retentions compared to methanol. Octylbenzene, decylbenzene and compound H1 were all affected by the displacement effect caused by the strongly adsorbing methanol acting as a displacing agent, resulting in distorted, compressed band profiles and anomalous efficiency. Compound H2 was affected by the tag-along effect caused by the abundance of methanol acting as an inhibitor, resulting in elongated peak shapes and decreased efficiency.

Conflict of interest

None.

Acknowledgements

The work was supported by the NKFIH OTKA grant K125312 and by grant GINOP-2.3.2-15-2016-00022.

We thank Dr. Abhijit Tarafder and Waters Corporation (Milford, MA,USA) for the long-term generous free loan of the ACQUITY UPC^2 equipment and for the support for accurate mass flow measurements.

References

[1] J. Yang, L. Zhu, Y. Zhao, Y. Xu, Q. Sun, S. Liu, C. Liu, B. Ma, Separation of furostanol saponins by supercritical fluid chromatography, J. Pharm. Biomed. Anal. 145 (2017) 71–78.
[2] I. Pfeifer, A. Murauer, M. Ganzera, Determination of coumarins in the roots of *Angelica dahurica* by supercritical fluid chromatography, J. Pharm. Biomed. Anal. 129 (2016) 246–251.
[3] G. Guiochon, A. Tarafder, Fundamental challenges and opportunities for preparative supercritical fluid chromatography, J. Chromatogr. A 1218 (2011) 1037–1114.
[4] A. Rajendran, Design of preparative-supercritical fluid chromatography, J. Chromatogr. A 1250 (2012) 227–249.
[5] L. Miller, Preparative enantioseparations using supercritical fluid chromatography, J. Chromatogr. A 1250 (2012) 250–255.
[6] C. Berger, M. Perrut, Preparative supercritical fluid chromatography, J. Chromatogr. A 505 (1990) 37–43.
[7] V. Desfontaine, A. Tarafder, J. Hill, J. Fairchild, A.G.-G. Perrenoud, J.-L. Veuthey, D. Guillarme, A systematic investigation of sample diluents in modern supercritical fluid chromatography, J. Chromatogr. A 1511 (2017) 122–131.
[8] T.A. Berger, Effect of density on kinetic performance in supercritical fluid chromatography with methanol modified carbon dioxide, J. Chromatogr. A 1564 (2018) 188–198.
[9] E. Glenne, H. Leek, M. Klarqvist, J. Samuelsson, T. Fornstedt, Systematic investigations of peak deformations due to co-solvent adsorption in preparative supercritical fluid chromatography, J. Chromatogr. A 1496 (2017) 141–149.
[10] E. Glenne, K. Öhlén, H. Leek, M. Klarqvist, J. Samuelsson, T. Fornstedt, A closer study of methanol adsorption and its impact on solute retentions in supercritical fluid chromatography, J. Chromatogr. A 1442 (2016) 129–139.
[11] V. Pauk, K. Lemr, Forensic applications of supercritical fluid chromatography – mass spectrometry, J. Chromatogr. B 1086 (2018) 184–196.
[12] A. Bajtai, G. Lajkó, I. Szatmári, F. Fülöp, W. Lindner, I. Ilisz, A. Péter, Dedicated comparisons of diverse polysaccharide- and zwitterionic cinchona alkaloid-based chiral stationary phases probed with basic and ampholytic indole analogs in liquid and subcritical fluid chromatography mode, J. Chromatogr. A 1563 (2018) 180–190.
[13] V. Desfontaine, D. Guillarme, E. Francotte, L. Nováková, Supercritical fluid chromatography in pharmaceutical analysis, J. Pharm. Biomed. Anal. 113 (2015) 56–71.
[14] J.L. Bernal, M.T. Martín, L. Toribio, Supercritical fluid chromatography in food analysis, J. Chromatogr. A 1313 (2013) 24–36.
[15] A. Tarafder, Metamorphosis of supercritical fluid chromatography to SFC: an overview, TrAC Trends Anal. Chem. 81 (2016) 3–10.
[16] F. Gritti, Unexpected retention and efficiency behaviors in supercritical fluid chromatography: a thermodynamic interpretation, J. Chromatogr. A 1468 (2016) 209–216.
[17] L.B. Nilsson, D. Westerlund, Peak compression effects in ion-pair reversed-phase liquid chromatography of substituted benzamides, Anal. Chem. 57 (1985) 1835–1840.
[18] M. Enmark, D. Åsberg, A. Shalliker, J. Samuelsson, T. Fornstedt, A closer study of peak distortions in supercritical fluid chromatography as generated by the injection, J. Chromatogr. A 1400 (2015) 131–139.
[19] G. Guiochon, A. Felinger, D.G. Shirazi, A.M. Katti, Fundamentals of Preparative and Nonlinear Chromatography, second ed., Academic Press, Amsterdam, 2006.
[20] M. Enmark, P. Forssén, J. Samuelsson, T. Fornstedt, Determination of adsorption isotherms in supercritical fluid chromatography, J. Chromatogr. A 1312 (2013) 124–133.
[21] A. Felinger, D. Zhou, G. Guiochon, Determination of the single component and competitive adsorption isotherms of the 1-indanol enantiomers by the inverse method, J. Chromatogr. A 1005 (2003) 35–49.
[22] A. Felinger, A. Cavazzini, G. Guiochon, Numerical determination of the competitive isotherm of enantiomers, J. Chromatogr. A 986 (2003) 207–225.
[23] A. Cavazzini, A. Felinger, G. Guiochon, Comparison between adsorption isotherm determination techniques and overloaded band profiles on four batches of monolithic columns, J. Chromatogr. A 1012 (2003) 139–149.
[24] J. Samuelsson, T. Undin, A. Törncrona, T. Fornstedt, Improvement in the generation of adsorption isotherm data in the elution by characteristic points method – the ECP-slope approach, J. Chromatogr. A 1217 (2010) 7215–7221.
[25] J. Samuelsson, T. Fornstedt, Injection technique for generating accurate adsorption isotherm data using the elution by characteristic points method, Anal. Chem. 80 (2008) 7887–7893.
[26] E. Forss, D. Haupt, O. Stålberg, M. Enmark, J. Samuelsson, T. Fornstedt, Chemometric evaluation of the combined effect of temperature, pressure, and co-solvent fractions on the chiral separation of basic pharmaceuticals using actual vs set operational conditions, J. Chromatogr. A 1499 (2017) 165–173.
[27] P. Vajda, G. Guiochon, Determination of the column hold-up volume in supercritical fluid chromatography using nitrous-oxide, J. Chromatogr. A 1309 (2013) 96–100.